WRF-based assessment of the Great Lakes' impact on cold season synoptic cyclones

Chuliang Xiao[1*], Brent M. Lofgren[2], and Jia Wang[2]

[1]*Cooperative Institute for Great Lakes Research (CIGLR), University of Michigan, Ann Arbor, Michigan, USA*

[2]*NOAA Great Lakes Environmental Research Laboratory, Ann Arbor, Michigan, USA*

Highlights:

#1: The Great Lakes generally strengthens the low pressure in winter near the surface but is sensitive to the background flow.

#2: The lake-air temperature gradient and surface wind controls the vertical heat flux.

#3: The meso-to-synoptic scale interaction should be taken into account when considering the Great Lakes' influence.

*Corresponding author address:

Chuliang Xiao, Ph. D.

Cooperative Institute for Great Lakes Research (CIGLR)

University of Michigan, Ann Arbor

4840 S. State Rd., Ann Arbor, MI 48108, USA

E-mail: cxiao@umich.edu

553 Laurentian Great Lakes: Physical drivers. Limnology and Oceanography 61, 1762-1786.
554 Xiao, C., B. M. Lofgren, J. Wang, et al., 2016. Improving the lake scheme within a coupled
555 WRF-lake model in the Laurentian Great Lakes. J. Adv. Model. Earth Syst. 8, 1969–1985,
556 doi:10.1002/2016MS000717.
557

List of Tables and Figures

Table 1. The detailed modification of land use, vegetation fraction, and soil category in NOLakes experiments, which is compared with the CONTROL experiments.

Fig. 1. The model domain with modified MODIS land categories. The Lake Superior is replaced by mixed forest and the other four lakes by cropland. The solid rectangle is used for area mean (see text in section 2.3). The lateral buffer zone is marked with dots.

Fig. 2. Surface maps of case 2009 at (a) 09 December and (b)10 December; case 2008 at (a) 14 December and (b) 15 December; case 2006 at (e) 01 December and (f) 02 December; case 2013 at (g) 14 December and (h) 15 December. The red contour denotes the sea level pressure (hPa). (Courtesy http://www.wpc.ncep.noaa.gov/archives/web_pages/sfc/sfc_archive_maps.php)

Fig. 3. Evolution of cyclones. The outlines of 996-hPa isobar of sea level pressure in UTC times for (a) case 2009 and (c) case 2006, and 1012-hPa isobar for (b) case 2008 and (d) case 2013. The low centers are marked with hrZdy (UTC time).

Fig. 4. The horizontal distribution of surface wind field at 10 m (vector, m s^{-1}), air temperature at 2 meters (shading, °C), and sea level pressure (contour, gpm) in (a) CONTROL, and (b) NARR for case 2009. (c) and (d) are for case 2008. (e) and (f) are for case 2006. (g) and (h) are for case 2013.

Fig. 5. (a) Simulated daily precipitation (mm) in WRF CONTROL experiment, compared with (b) NARR and (c) CPC unified gauged-based analysis for case 2009. (d), (e) and (f) are for case 2008. (g), (h) and (i) are for case 2006. (j), (k) and (l) are for case 2013.

Fig. 6. Evolutions of area-mean SLP (hPa) for (a) case 2009, (b) case 2008, (c) case 2006, and (d) case 2013. The CONTROL and NOLakes experiments are denoted red and blue curves,

580 respectively, compared with the NARR in dash. The bottom bar represents the enhancement ratio
581 (see text for definition).

582 **Fig. 7.** (a) Lake-mean surface temperature (TSK, °C), (b) area-mean air temperature at 2 m
583 (T2m, °C), and (c) the difference (T2m-TSK) for case 2009. (d), (e) and (f) for case 2008. (g), (h)
584 and (i) for case 2006. (j), (k) and (l) for case 2013. The CONTROL and NOLakes experiments
585 are denoted as black and red curves, respectively.

586 **Fig. 8**. Simulated latent heat flux (red) in case 2013, compared with the eddy covariance
587 observation (black) in Stannard Rock station in Lake Superior.

588 **Fig. 9.** Daily mean sensible heat flux (SH) and latent heat flux (LH) (W m^{-2}) in CONTROL
589 experiments and NOLakes experiments. (a), (b), (c) and (d) are for case 2009. (e), (f), (g) and (h)
590 are for case 2008. (i), (j), (k) and (i) are for case 2006. (m), (n), (o) and (p) are for case 2013.

591 **Fig. 10.** Surface moisture flux (vector, g kg^{-1} m s^{-1}) and its divergence (shading, 10^{-6} g kg^{-1} s^{-1}) of
592 (a) CONTROL, (b) NOLakes, and (c) the difference (CONTROL – NOLakes) for case 2009. (d),
593 (e) and (f) are for case 2008. (g), (h) and (i) are for case 2006. (j), (k) and (l) are for case 2013.

594 **Fig. 11.** Southwest-northeast vertical cross sections of geopotential height (contour, gpm) and
595 potential temperature (shading, K) in (a) CONTROL, and (b) the difference (CONTROL –
596 NOLakes) for case 2009. (c) and (d) for case 2008. (e) and (f) for case 2006. (g) and (h) for case
597 2013. The thick solid line in the bottom of each panel represents the portion of the cross section
598 covering the rectangular region in Fig. 1.

599 **Fig. 12.** The horizontal distribution of surface wind field at 10 m (vector, m s^{-1}), temperature at
600 850 hPa (shading, °C), and geopotential height at 500 hPa (contour, gpm) in (a) case 2009, (c)
601 case 2008, (e) case 2006, and (g) case 2013. (b), (d), (f) and (h) are the same as (a), (c), (e), and
602 (g), but for the difference (CONTROL – NOLakes), respectively.

603 **Fig. 13.** The area-mean absolute vorticity (solid line, 10^{-5} s^{-1}) and the portion of the vorticity
604 trend (dash line, 10^{-11} s^{-2}) from heat and friction at 300 K isentropic level for (a) case 2009, (b)
605 case 2008, (c) case 2006, and (d) case 2013.

606 Table 1. The detailed modification of land use, vegetation fraction, and soil category in NOLakes
607 experiments, which is compared with the CONTROL experiments.

Variable Description	Variable Name	CONTROL	NOLakes	
			Superior	Others
Land use	LU_INDEX	Water Bodies	Mixed Forest	Cropland
Vegetation fraction	VEGFRA	0%	20%	25%
Soil category	SOILCTOP SOILCBOT	Water	Sandy Loam	Silt Loam

608

609

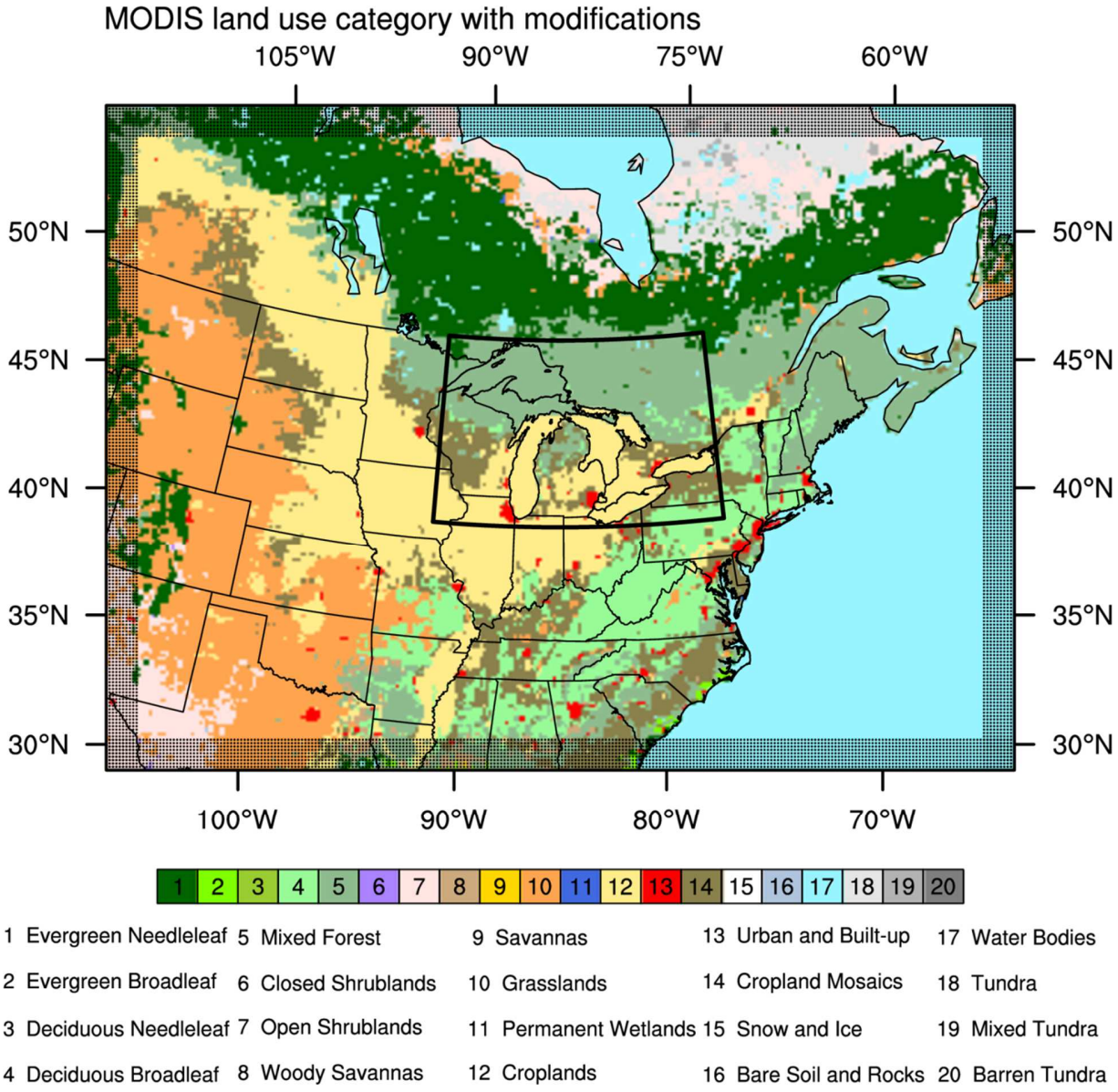

610

611 **Fig. 1.** The model domain with modified MODIS land categories. The Lake Superior is replaced

612 by mixed forest and the other four lakes by cropland. The solid rectangle is used for area mean

613 (see text in section 2.3). The lateral buffer zone is marked with dots.

614

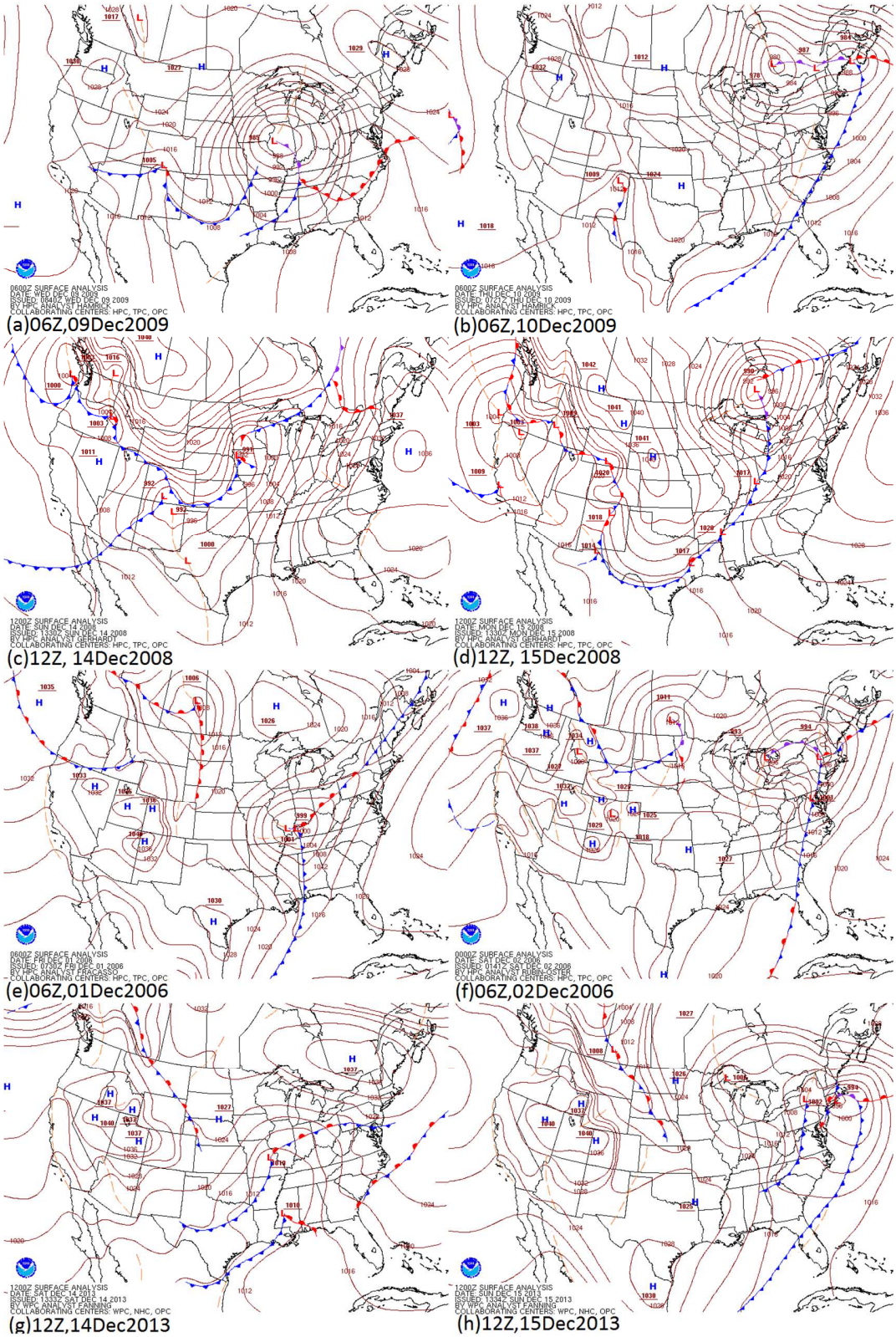
(a)06Z,09Dec2009
(b)06Z,10Dec2009
(c)12Z, 14Dec2008
(d)12Z, 15Dec2008
(e)06Z,01Dec2006
(f)06Z,02Dec2006
(g)12Z,14Dec2013
(h)12Z,15Dec2013

615

616 **Fig. 2.** Surface maps of case 2009 at (a) 09 December and (b)10 December; case 2008 at (a) 14
617 December and (b) 15 December; case 2006 at (e) 01 December and (f) 02 December; case 2013
618 at (g) 14 December and (h) 15 December. The red contour denotes the sea level pressure (hPa).
619 (Courtesy http://www.wpc.ncep.noaa.gov/archives/web_pages/sfc/sfc_archive_maps.php)

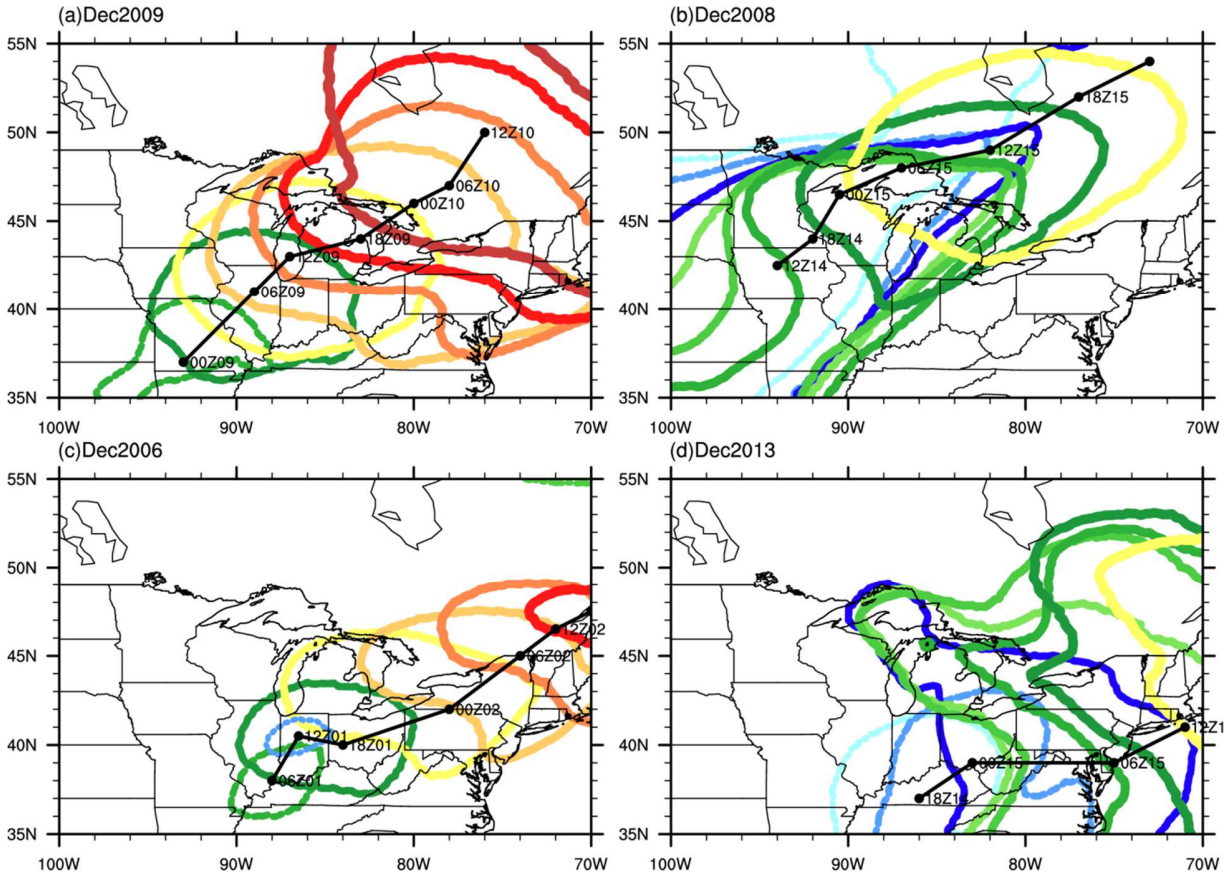

Fig. 3. Evolution of cyclones from NARR. The outlines of 996-hPa isobar of sea level pressure in UTC times for (a) case 2009 and (c) case 2006, and 1012-hPa isobar for (b) case 2008 and (d) case 2013. The low centers are marked with hrZDD (UTC time of the day).

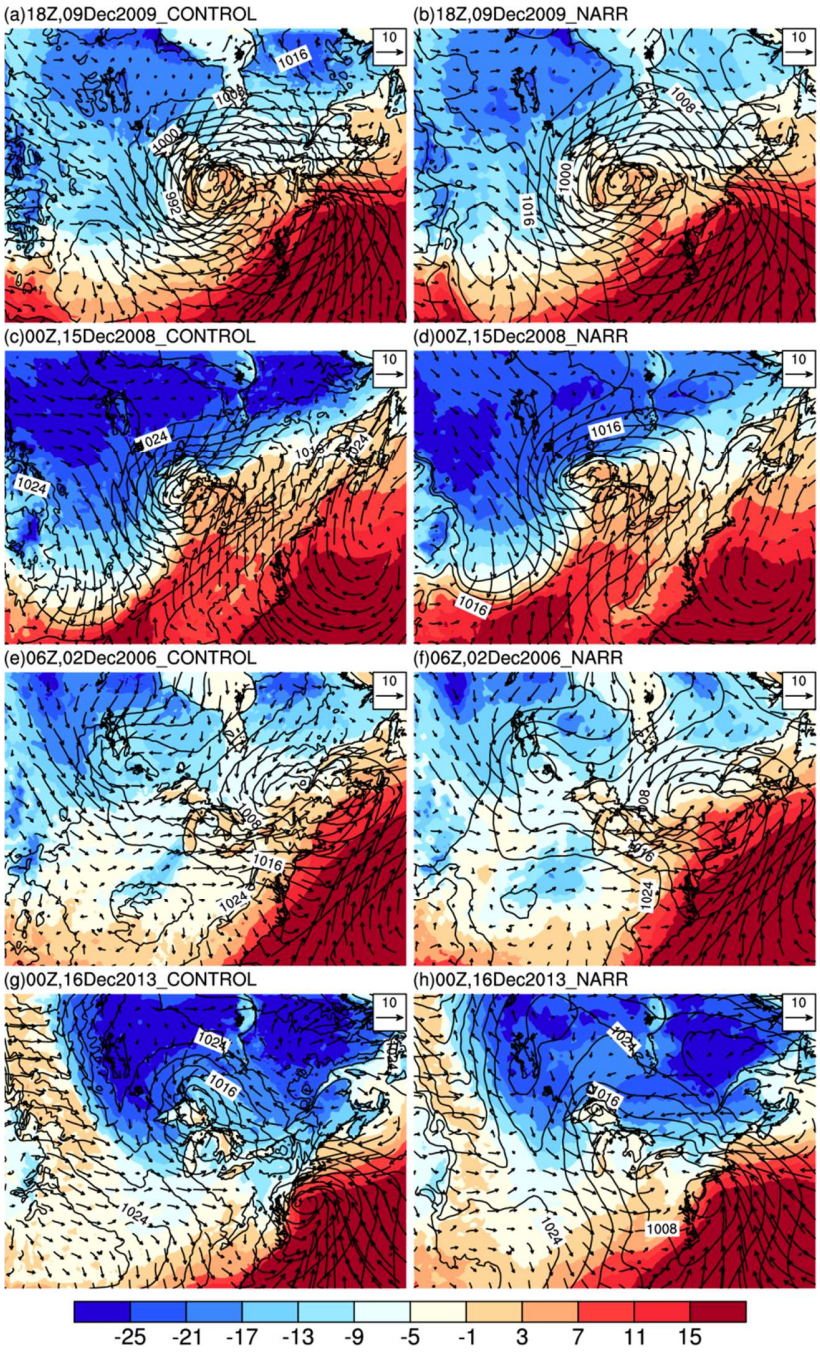

625

626 **Fig. 4.** The horizontal distribution of surface wind field at 10 m (vector, m s^{-1}), air temperature at

627 2 meters (shading, °C), and sea level pressure (contour, hPa) for (a, c, e, g) CONTROL and (b, d,

628 f, h) NARR for cyclone case studies in (a, b) 2009, (c, d) 2008, (e, f) 2006, and (g, h) 2013.

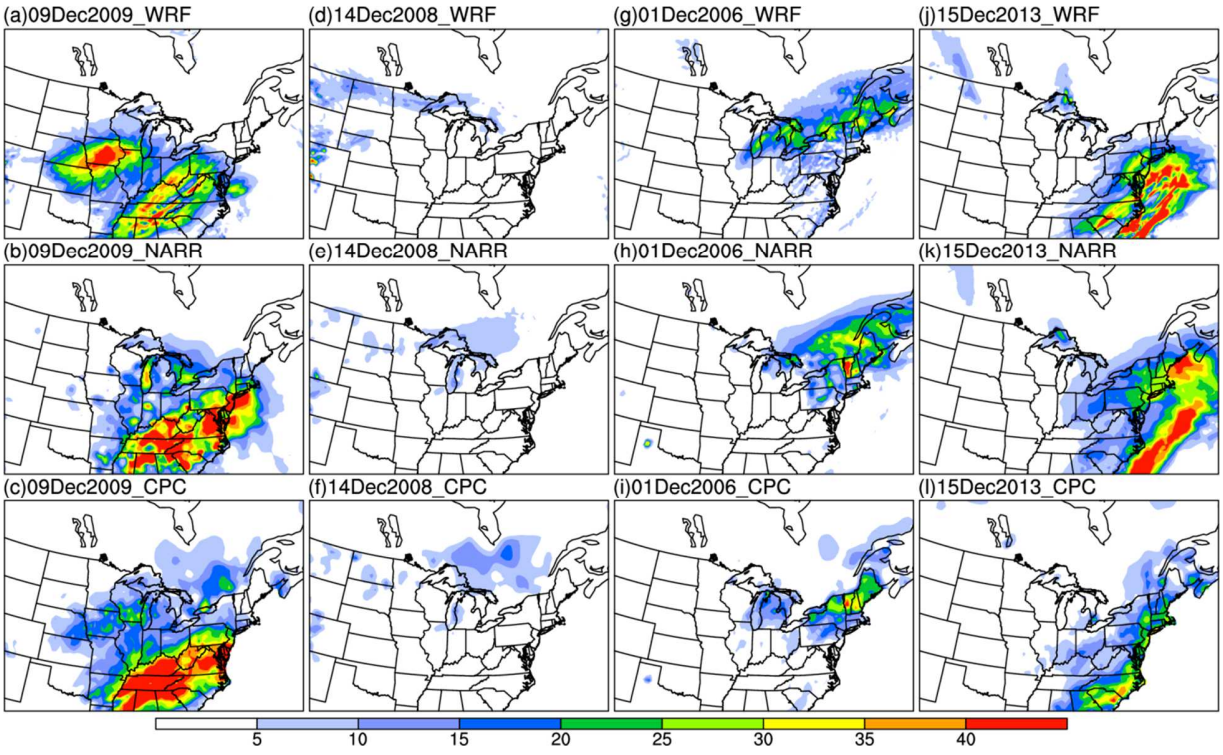

629

630 **Fig. 5.** (a) Simulated daily precipitation (mm) in WRF CONTROL experiment, compared with

631 (b) NARR and (c) CPC unified gauged-based analysis for case 2009. (d), (e) and (f) are for case

632 2008. (g), (h) and (i) are for case 2006. (j), (k) and (l) are for case 2013.

633

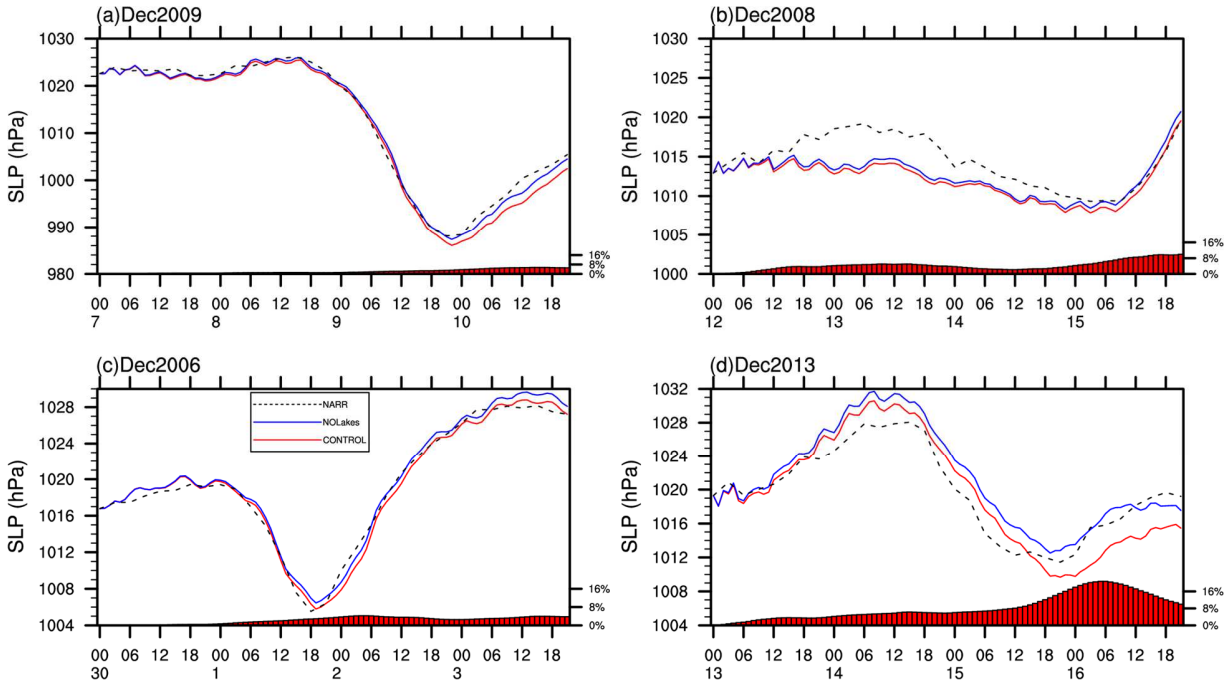

634

635 **Fig. 6.** Evolutions of area-mean SLP (hPa) for (a) case 2009, (b) case 2008, (c) case 2006, and (d)
636 case 2013. The CONTROL and NOLakes experiments are denoted by red and blue curves,
637 respectively, compared with the NARR in dash. The bottom bars represent the enhancement ratio
638 (see text for definition).

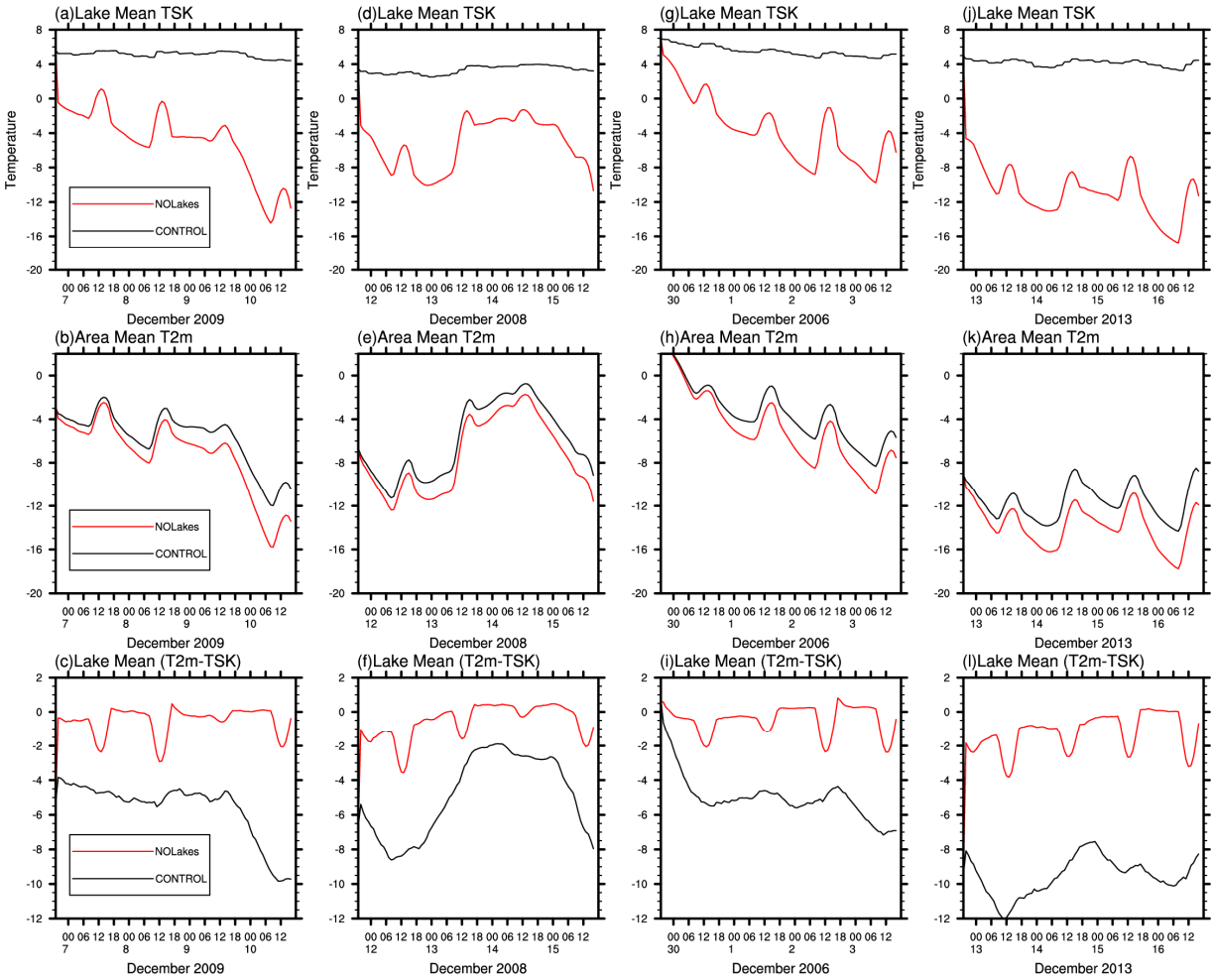

Fig. 7. (a) Lake-mean surface temperature (TSK, °C), (b) area-mean air temperature at 2 m (T2m, °C), and (c) the difference (T2m-TSK) for case 2009. (d), (e) and (f) for case 2008. (g), (h) and (i) for case 2006. (j), (k) and (l) for case 2013. The CONTROL and NOLakes experiments are denoted as black and red curves, respectively.

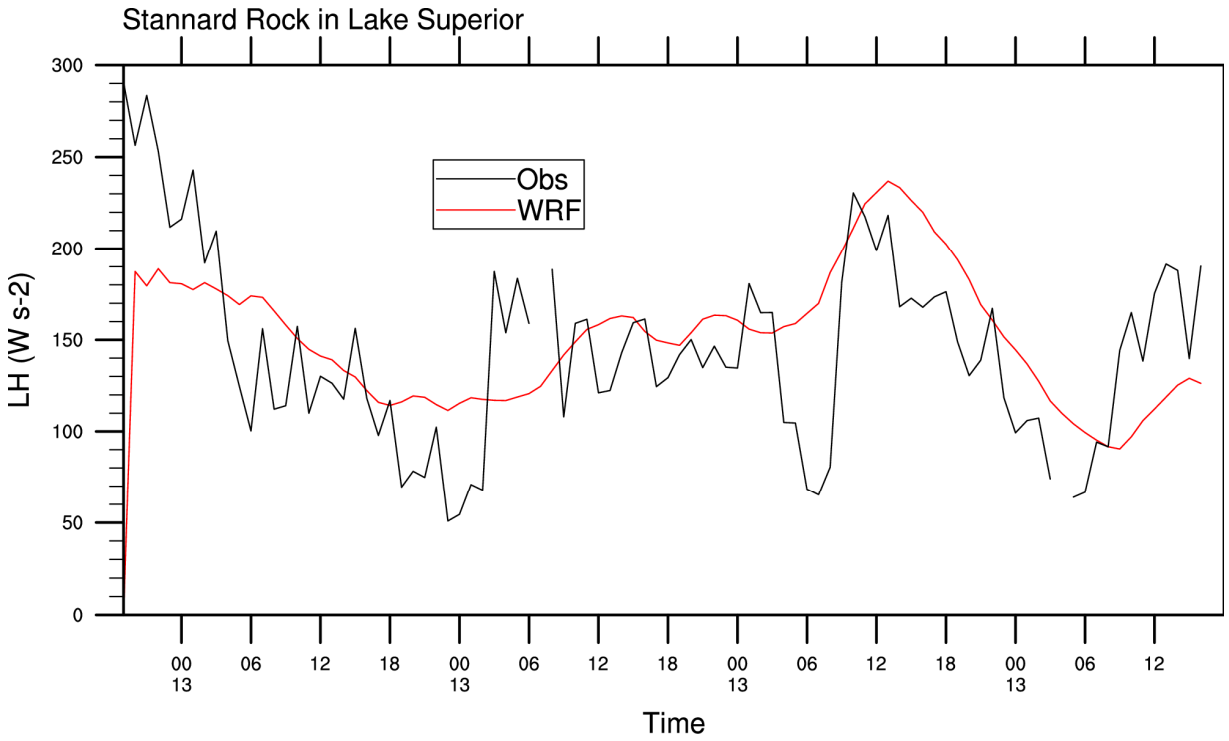

Fig. 8. Simulated latent heat flux (red) in case 2013, compared with the eddy covariance observation (black) in Stannard Rock station in Lake Superior.

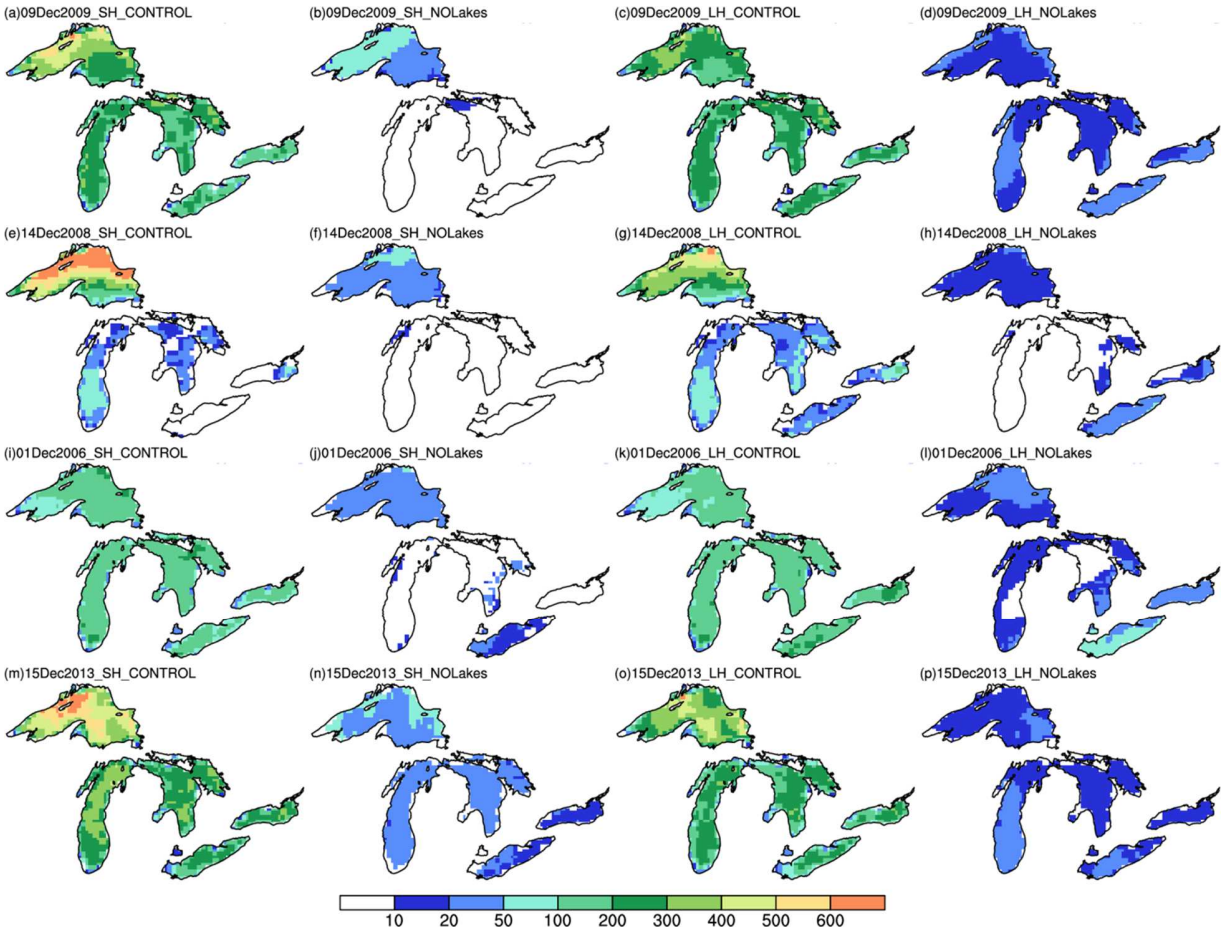

649

650 **Fig. 9.** Daily mean sensible heat flux (SH) and latent heat flux (LH) (W m^{-2}) in CONTROL
651 experiments and NOLakes experiments. (a), (b), (c) and (d) are for case 2009. (e), (f), (g) and (h)
652 are for case 2008. (i), (j), (k) and (i) are for case 2006. (m), (n), (o) and (p) are for case 2013.

653

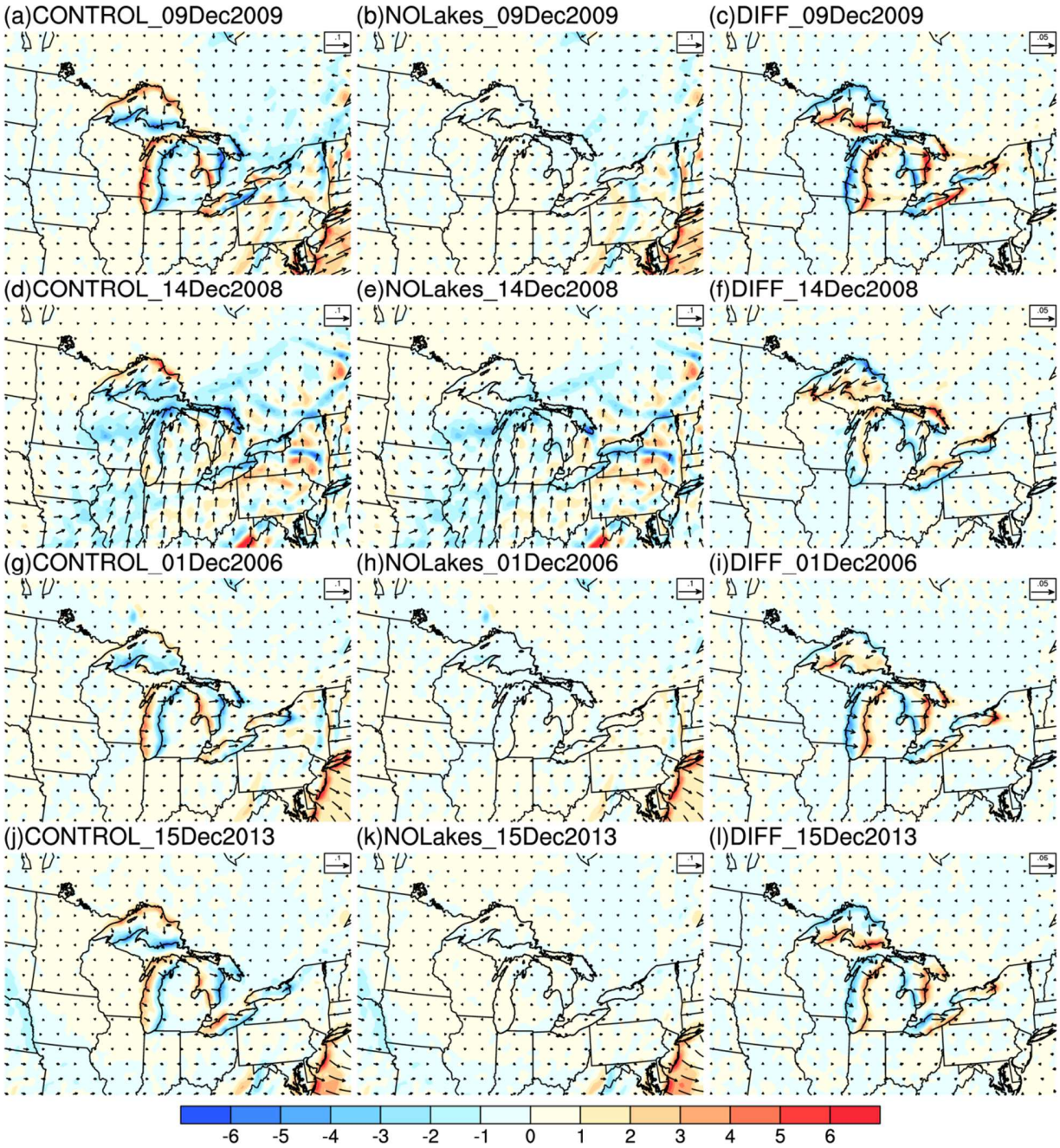

654

655 **Fig. 10.** Surface moisture flux (vector, g kg^{-1} m s^{-1}) and its divergence (shading, 10^{-6} g kg^{-1} s^{-1}) of

656 (a) CONTROL, (b) NOLakes, and (c) the difference (CONTROL – NOLakes) for case 2009. (d),

657 (e) and (f) are for case 2008. (g), (h) and (i) are for case 2006. (j), (k) and (l) are for case 2013.

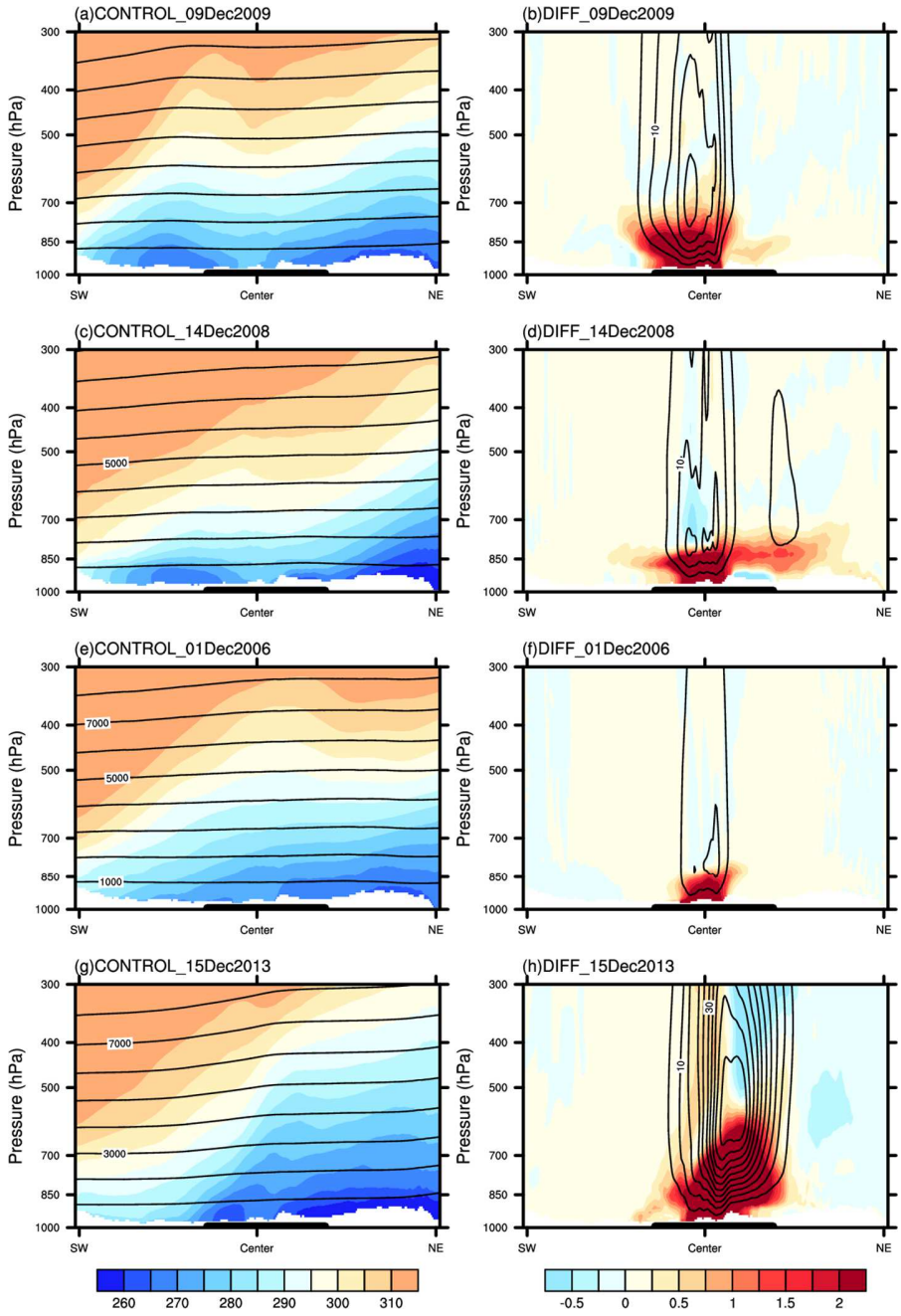

658

659 **Fig. 11.** Southwest-northeast vertical cross sections of geopotential height (contour, gpm) and
660 potential temperature (shading, K) in (a) CONTROL, and (b) the difference (CONTROL –
661 NOLakes) for case 2009. (c) and (d) for case 2008. (e) and (f) for case 2006. (g) and (h) for case
662 2013. The thick solid line in the bottom of each panel represents the portion of the cross section
663 covering the rectangular region in Fig. 1.

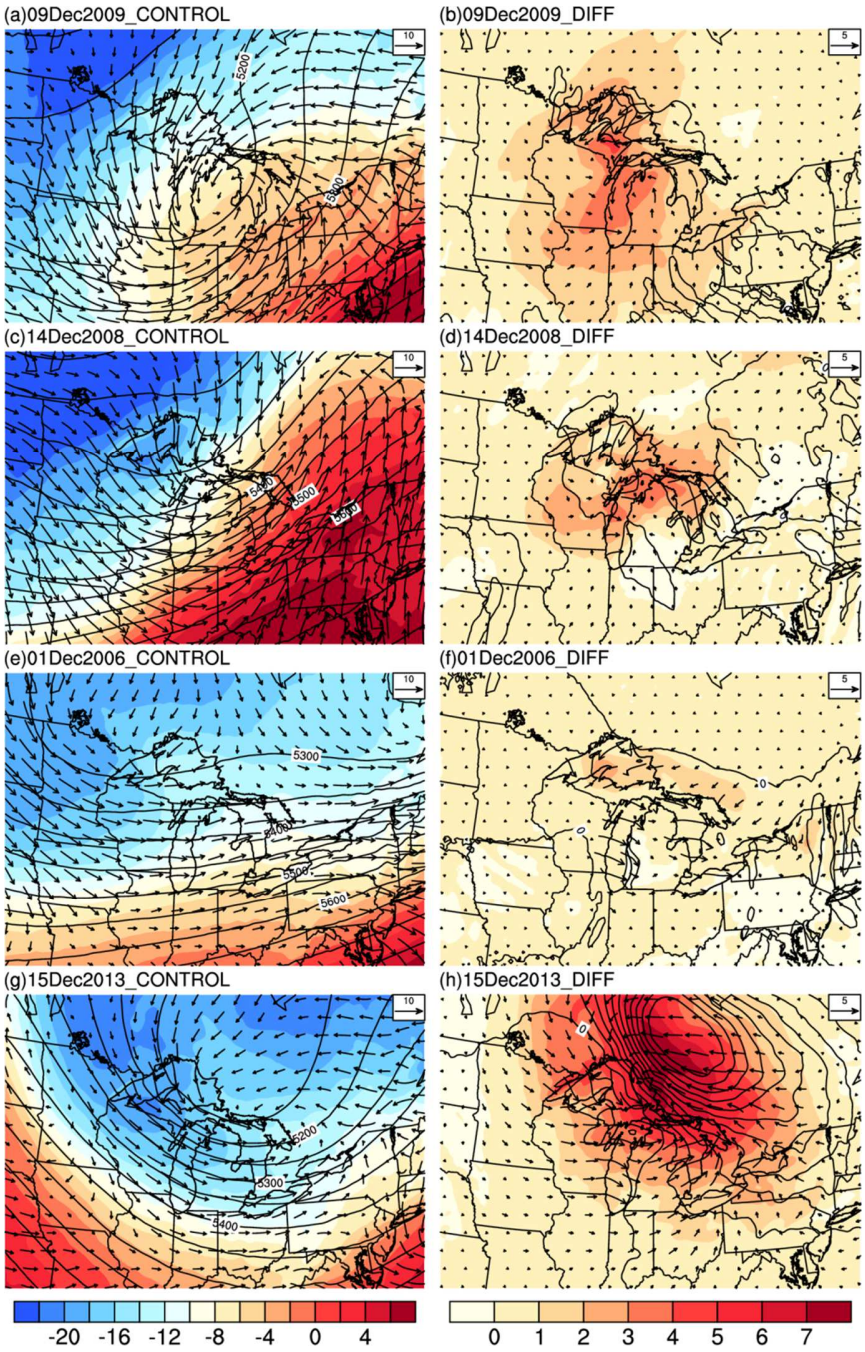

664

665 **Fig. 12.** The horizontal distribution of surface wind field at 10 m (vector, m s^{-1}), temperature at

666 850 hPa (shading, °C), and geopotential height at 500 hPa (contour, gpm) in (a) case 2009, (c)

667 case 2008, (e) case 2006, and (g) case 2013. (b), (d), (f) and (h) are the same as (a), (c), (e), and

668 (g), but for the difference (CONTROL – NOLakes), respectively.

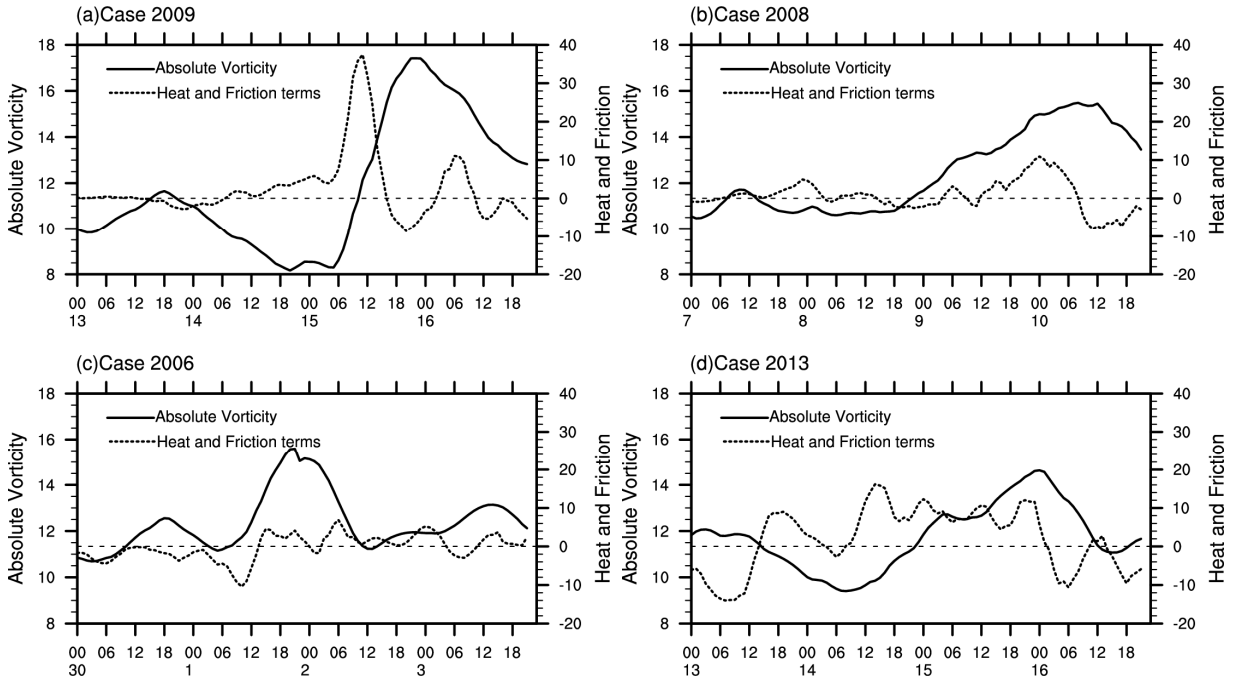

669

670 **Fig. 13.** The area-mean absolute vorticity (solid line, 10^{-5} s^{-1}) and the portion of the vorticity

671 trend (dash line, 10^{-11} s^{-2}) from heat and friction contributed by lakes (CONTROL – NOLakes) at

672 300 K isentropic level for (a) case 2009, (b) case 2008, (c) case 2006, and (d) case 2013.